ARTICLE

# Electric-Field-Assisted Dip-Pen Nanolithography on Poly(4-vinylpyridine) (P4VP) Thin Films

**Xiaohua Wang,[†] Xin Wang,[‡] Rodolfo Fernandez,[†] Leonidas Ocola,[§] Mingdi Yan,[*,‡] and Andres La Rosa[*,†]**

Department of Physics and Department of Chemistry, Portland State University, Portland, Oregon 97201, United States, and Center for Nanoscale Materials, Argonne National Laboratory, 9700 South Cass Avenue, Building 440, Argonne, Illinois 60439, United States

**ABSTRACT** Dip-pen nanolithography (DPN) has attracted increased attention for its ability to generate nanometer-scale patterns on solid surface using an "ink"-coated atomic force microscope (AFM) tip. In contrast to this conventional anchoring-molecules procedure, nanopatterns can also be created by triggering the structural response of the proper substrate. In one approach, the delivery of acidic buffer from the tip into a poly(4-vinylpyridine) (P4VP) thin film (while the tip is being laterally moved, in a raster fashion, along a preprogrammed pattern) leads to the polymer swelling in response to the local protonation. This practice, however, has suffered from a lack of consistency due to the potentially many factors influencing the pattern formation. Herein we report that a more reliable strategy for well controlling the protonation process results when applying an electric field between the AFM tip and the sample. We demonstrate the improved capabilities of the electric-field-assisted DPN method towards reproducibly and reliably fabricating nanostructures by taking advantage of the responsive characteristics (i.e. swelling) of P4VP. Our work includes a systematic study of pattern fabrication under different patterning parameters (mainly the applied bias and contact force) and, very important, provides evidence of the reversible characteristic of the pattern formation process.

**KEYWORDS:** cross-linked P4VP thin film • protonation • electric-field-assisted • erasable patterns • dip-pen nanolithography

## INTRODUCTION

Nanolithography comprises a set of technologies capable of etching, writing, or patterning materials with nanometer scale precision, which nowadays has widespread applications in electronic engineering, physics, chemistry, and biology. Nanolithography is the avenue for constructing nanoelectronic devices that take advantage of quantum mechanical phenomena, such as single-electron transistors (SETs), resonant tunneling diodes (RTDs) (1, 2), quantum dot lasers, and storage devices (3, 4). With the miniaturization trend in device size, nanolithography opens up opportunities for applications in diverse areas, such as nanoelectromechanical systems (NEMS) (5) and ultrasmall chemical and biochemical sensors (6). More recently, dip-pen nanolithography (DPN) has been introduced for fabricating nanostructures on solid surfaces (7).

DPN is used to directly deliver atoms or molecules (initially attached by adhesion to an atomic force microscope (AFM) tip) onto substrates of interest in a controlled fashion. A diverse range of molecular species such as small organic molecules (7), biological macromolecules (8), conducting polymers (9), metal ions, and nanoparticles (10, 11) have been deposited via DPN process onto surface of proper affinities. In addition, the patterning substrates have been expanded to include metals (12), insulators (12), semiconducting materials (13), and functional monolayers adsorbed on substrates (14). Applications of DPN have been envisioned in nanoelectronics (15), microfluidics (16), molecular electronics (organic circuits) (17), and nanosensors for biological and chemical species (18), etc. In most cases, the transport of "ink" molecules from the tip to the substrate occurs in a liquid bridge naturally formed between them through capillary condensation. Hence, this technique has also been used to experimentally study the mechanism of molecular diffusion through nanoscale junctions and the in situ growth of self-assembled monolayers under ambient conditions (19, 20). Furthermore, due to its direct-write capability, DPN is suitable for investigating responsive films at the mesoscopic scale.

Responsive films made of self-assembled monolayers (SAMs) or polymer thin films are valuable in the development of electronic, analytical and biomedical devices. These films exhibit different properties in response to external signals, such as the changes in temperature, pH, light, and ionic strength. Poly(4-vinylpyridine) (P4VP), a weak polyelectrolyte, can be prepared as polymer thin films tethered to solid supports simply by spin coating and subsequent UV irradiation (21). The immobilization results from the UV induced cross-linking of polymer leading to the attachment of polymer film to the substrate. Moreover, P4VP film shows

* Corresponding author. E-mail: yanm@pdx.edu, (M.Y.); andres@pdx.edu (A.L.).
Received for review July 8, 2010 and accepted September 21, 2010
[†] Department of Physics, Portland State University.
[‡] Department of Chemistry, Portland State University.
[§] Argonne National Laboratory.
DOI: 10.1021/am1005964
2010 American Chemical Society

a pH-dependent response that causes the structural changes of the polymer and controls surface wettability (22). The reversible transformation of P4VP originates from the protonation of pyridine units in the polymer, thus providing the basis for applications of P4VP films as responsive coatings. Recently, P4VP polymer-brush-functionalized electrodes have been designed for future "smart" bioelectronic devices ranging from biosensors to biofuel cells (23, 24). Additionally, P4VP is an interesting material because of its tunable photoluminescence (PL) properties. Vaganova et al. demonstrated that P4VP with protonated polymeric pyridine groups displayed photoactive emission properties, which could be tuned to glow blue, red, or green, depending on the pumping wavelength (25).

We have previously demonstrated the fabrication of patterns on P4VP thin films based on the DPN technique (26, 27). Differing from the conventional feature formation via a direct deposition of ink molecules onto substrates, the underlying working principle in our approach constitutes the delivery of hydronium ions from the sharp tip into the polymer thin film, which leads to the polymer swelling in response to the local protonation. The process, however, has suffered from a lack of consistency due to the potentially many factors intervening in the pattern formation (sometimes very clear patterns were formed; but in other occasions and under apparently similar conditions, no pattern was formed at all). Herein we report an alternative strategy for reliably attaining patterns formation by applying an electric field between the AFM tip and the sample. We demonstrate the improved capabilities of this electric-field-assisted DPN technique towards reproducibly and reliably fabricating nanostructures taking advantage of the responsive characteristics (swelling) of P4VP films. Our work includes a systematic study of pattern formation under different patterning parameters (mainly the externally applied bias and the tip-sample contact force). More importantly, the patterns can be erased, and evidence is provided on the reversible characteristic of this process.

## EXPERIMENTAL SECTION

**Polymer Thin Film Preparation.** P-type silicon (100) wafers were cleaned by immersion in piranha solution, composed of 35% hydrogen peroxide ($H_2O_2$) and 98% sulfuric acid ($H_2SO_4$) in the ratio of 3:7 by volume, stirring for 60 min at 80−90°C to remove contaminants (**Caution**: *the piranha solution reacts violently with many organic solvents.*). Subsequently, the silicon wafers were washed with boiling water for 90 min, and then dried under $N_2$. The clean wafers were then dipped into HF aqueous solution to remove the native oxide layer from the silicon surface, rinsed thoroughly with Milli-Q water, and dried with $N_2$. A solution of P4VP (molecular weight ca. 160 000) in *n*-butanol (10 mg/mL) was spin-coated onto silicon substrates at 2000 rpm for 60 s. The polymer-coated substrates were irradiated with a 450 W medium-pressure mercury lamp for 15 minutes (the irradiation time included approximate 2 minutes warm up for the UV lamp to reach its maximal intensity). The unbound polymers were removed by soaking the irradiated samples in *n*-butanol for 12 h. The remaining films were dried with $N_2$, and the thickness was measured on a Gaertner Model L116A ellipsometer with a 632.8 nm He/Ne laser at an incident angle of 70°. The refractive index used in the model to determine the film thickness was 1.581 for P4VP. An average thickness of 40 nm was obtained after taking measurements at three different locations.

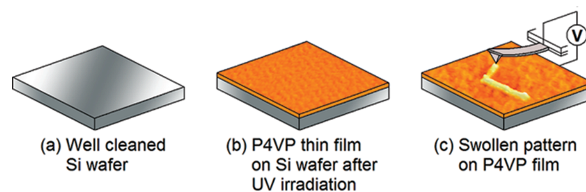


**FIGURE 1. Scheme of the experimental sequence: (a) freshly cleaned silicon wafer; (b) polymer film attached to the silicon wafer after UV radiation; and (c) patterning process while applying a bias voltage.**

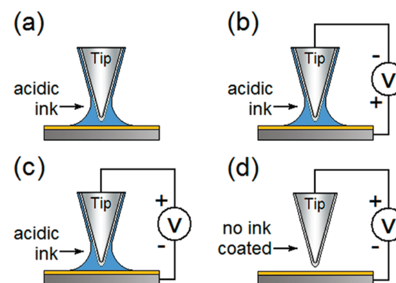


**FIGURE 2. Different experimental settings used for patterning features on P4VP polymer films: The tip inked with acidic buffer and (a) not biased, (b) negatively biased, (c) positively biased. (d) An uncoated tip positively biased.**

**Force Calibration.** Silicon-based AFM cantilevers of high spring constant coated with 15-nm thick wear-resistant platinum (NSC15/Pt, $k = 40$ N/m, MikroMasch) were used for surface patterning and imaging. The normal spring constant of each cantilever was calibrated using the Sader method (28), which states the relation $k = 0.1906\rho_f b^2 L Q_f \omega_f^2 \Gamma_i^f(\omega_f)$, where $L$ and $b$ are the length and width of the cantilever, respectively, $\rho_f$ is the density of air (1.18 kg/m$^3$ at 25°C), $\omega_f$ and $Q_f$ are the resonance frequency and quality factor of the fundamental resonance peak in air, respectively, and $\Gamma_i^f$ is the imaginary part of the hydrodynamic function.

**Pattern Formation and Characterization.** All the experiments presented below were performed with a commercial AFM (XE-120, Park Systems) in an ambient environment (23−26°C and 45−55% relative humidity). Prior to the patterning process, the AFM tip was inked by dipping into a phosphate buffer solution for 1 min and blown dry with $N_2$. Buffer solutions (100 mM) of pH 4.0 and pH 8.3 were prepared by dissolving sodium dihydrogen phosphate ($NaH_2PO_4$) and sodium hydrogen phosphate ($Na_2HPO_4$) in the appropriate proportions in distilled water (13.8 and 0.036 g/L, respectively, for pH 4.0, and 0.489 and 25.9 g/L, respectively, for pH 8.3). The sample was grounded while a bias was applied to the tip. The voltages were quoted by referencing the polarity of the tip. The bias voltage was held constant while the tip transcribed the preprogrammed patterns controlled by the AFM in contact mode. To visualize the resulting patterns, we subsequently acquired topographic images by operating the AFM in noncontact mode with the same tip used for patterning. A scheme of the patterning process on P4VP thin film is shown in Figure 1.

## RESULTS AND DISCUSSION

As outlined in Figure 2, a series of systematic experiments were carried out to study the mechanism of pattern formation, as well as to explore the role played by externally applied bias voltages and tip-sample contact forces. The AFM

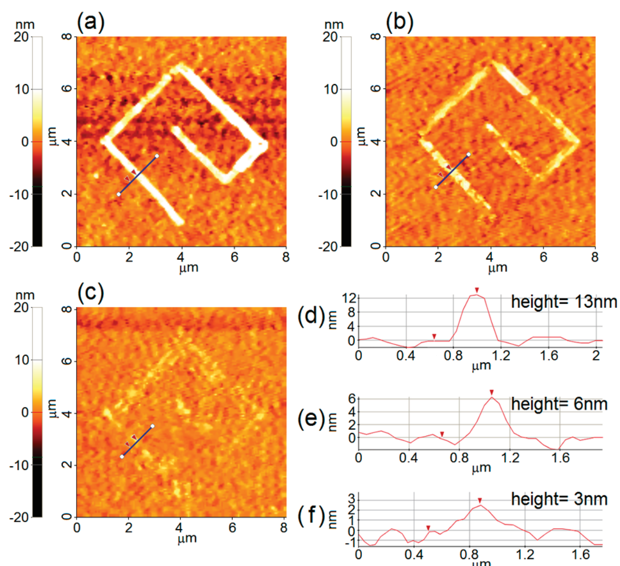


FIGURE 3. Topographic images (8 $\mu$m × 8 $\mu$m) of features drawn by applying a constant force of 1.0 $\mu$N. The applied bias voltages (V) and measured heights of selected lines (nm) are the following: (a) 5, 13; (b) 3, 6; and (c) 0, 3. Line profile plots of (d−f) correspond to the features selected in (a−c), respectively.

tip was immersed into the acidic phosphate buffer solution of pH 4.0. During the patterning operation, the inked tip was scanned across the polymer surface at a fixed writing speed of 80 nm/s, while the contact force between the tip and the surface was held constant. In previous experiments, we fabricated features using writing speeds up to 500 nm/s. The lower speed of 80 nm/s used in the present work was conservatively chosen in response to our focused interest in evaluating the effects of the applied bias and contact force on the patterning process, preventing possible interference in our results that might be associated to higher scanning speeds. The general results reported herein are that when no bias voltage was applied, the pattern formation was neither noticeable nor reproducible; when the tip was negatively biased, no structure formation was observed; by contrast, swollen patterns consisting of continuous lines were obtained when the tip was positively biased. Figure 3 shows topographic images and corresponding line profiles of structures created using a constant force of 1.0 $\mu$N and different bias voltages. The heights of the selected features on the images are found to be 13, 6, and 3 nm, corresponding to applied bias voltages of 5, 3, and 0 V, respectively. A similar trend of creating taller patterns with higher applied voltage was obtained when using different contact forces (0.8 and 0.5 $\mu$N), the experimental results are quantitatively and statistically summarized in Figure 4. The surface roughness obscured the observation of the potential pattern formation at the contact force of 0.5 $\mu$N and a bias of 0 V. Also, when the patterning operation was attempted using an uncoated tip, no swollen pattern could be obtained even if the tip was positively biased.

To examine the stability of patterned features, two images of the same area on the sample were taken 24 h apart; the results are shown in Figure 5 (Figure 5a was

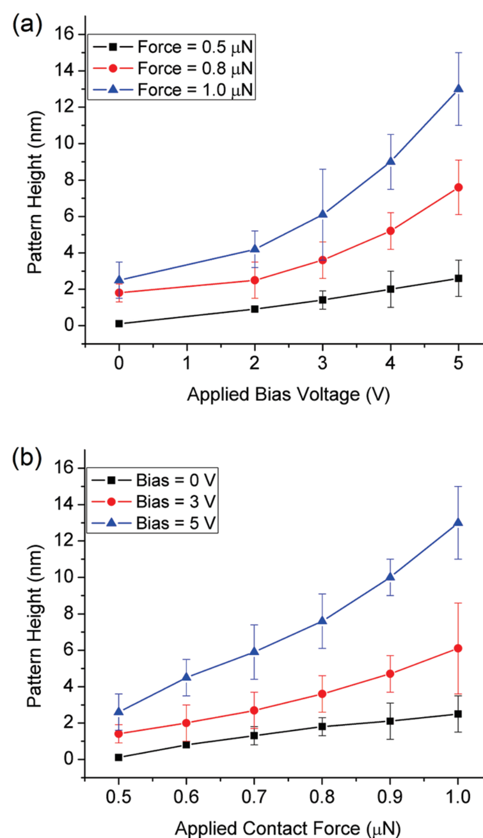


FIGURE 4. (a) Pattern height (nm) vs applied bias voltage (V) at various fixed contact forces. (b) The pattern height (nm) vs applied contact forces ($\mu$N) under different constant bias voltages. Each data point was the average of 3 measurements each on at least 10 line features created under the same conditions.

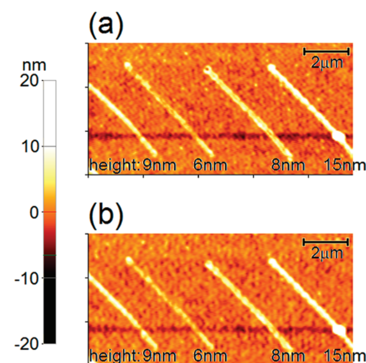


FIGURE 5. Images of the same sample region taken 24 h apart. The heights of lines (from left to right): 9 nm (1.0 $\mu$N, 4 V), 6 nm (1.0 $\mu$N, 3 V), 8 nm (1.0 $\mu$N, 4 V), and 15 nm (1.0 $\mu$N, 5 V) are not found to be altered. Each value was the average of 3 measurements on each line profile.

taken first). The line features were unaltered, suggesting that the patterns were not composed of volatile materials.

To further support the claim that the presence of raised patterns were a consequence of the swelling response of the P4VP polymer film (22, 26), we demonstrated the reversibility of the patterning process by selectively erasing an existing swollen pattern. "Dot" features were initially generated using a tip coated with the acidic ink. Only the dot at the center of Figure 6 (denoted by the dashed-line square) was then twice subjected to the "erasing" operation, which consisted of using the same tip but inked with a basic

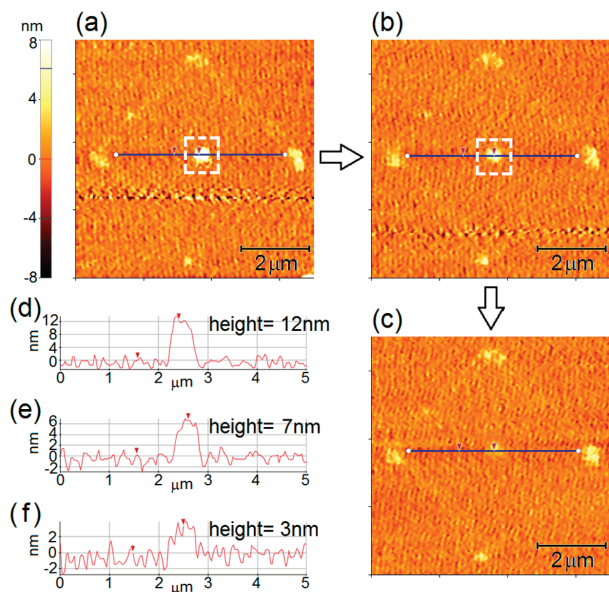


FIGURE 6. Topographic images show the removal of the dot pattern at the center: (a) Initial pattern. (b) After the first erasing step. (c) After the second erasing step. Line profile plots of (d−f) correspond to the features selected in (a−c), respectively.

phosphate buffer solution of pH 8.3 without applying the bias voltage. The removal of the existing dot was performed by keeping the tip in contact and stationary on top of the dot (no scanning movement). The images in Figure 6 show the progressive attenuation of the dot height, from 12 to 7 and finally to 3 nm. During the "erasing" process, the applied load exerted by the tip was kept intentionally low (i.e., 0.5 $\mu$N) so as to minimize potential damages to the dot pattern. As shown in Figure 7, there is indeed no change in the heights of "dot" features when the "erasing" experiment was attempted using an uncoated tip under the 0.5 $\mu$N load. This additional test rules out the possibility that the decrease in height might be caused by mechanical scratches on the feature. Altogether, the result indicates that the disappearance of the central dot in Figure 6 was not due to mechanical damages caused by the tip but to the presence of basic buffer solution neutralizing the protonated polymer, causing the deswelling of the film.

This technique was also capable of producing complex pattern shapes of sub-100 nm line-width. Line profiles of thickness as small as about 60 nm are displayed in Figure 8a, along with a pattern of the letters PSU (Figure 8b), in a 5 $\mu$m × 5 $\mu$m square region. In the latter, the average line width is about 180 nm.

Experimental results presented herein suggest that the working mechanism of pattern formation on the P4VP thin film is the local protonation of pyridine units of the polymer with the hydronium ions ($H_3O^+$). As outlined in Figure 9, the abundant $H_3O^+$ ions in the acidic ink delivered into the film cause the protonation of pyridine groups, whose Coulomb repulsions make the polymer swell (the counter ions, not shown in the figure, partially screening this interaction). This is further supported by our previous result obtained using Kelvin probe force microscopy revealing a lack of net charge in the swollen structures (27). Moreover, the decrease in height of a given existing feature upon the deposition of basic ink reveals that the swollen patterns are generated by polymer protonation rather than, for example, residual salt accumulation from the buffer solution. This observation also provides evidence of the reversible characteristic of the patterning process.

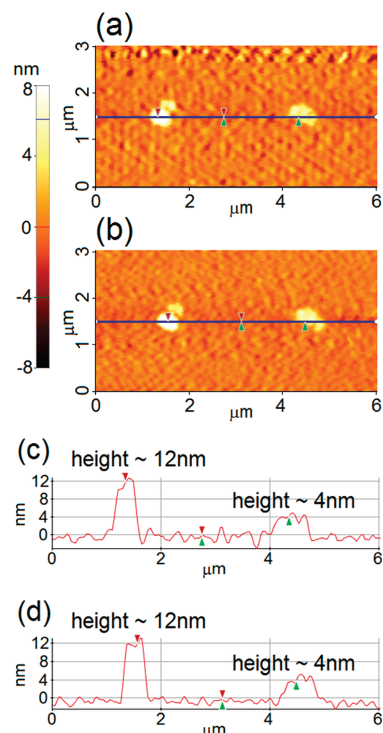


FIGURE 7. Topographic images taken (a) before and (b) after performing the "erasing" operation using an uncoated tip at the contact force of 0.5 $\mu$N.

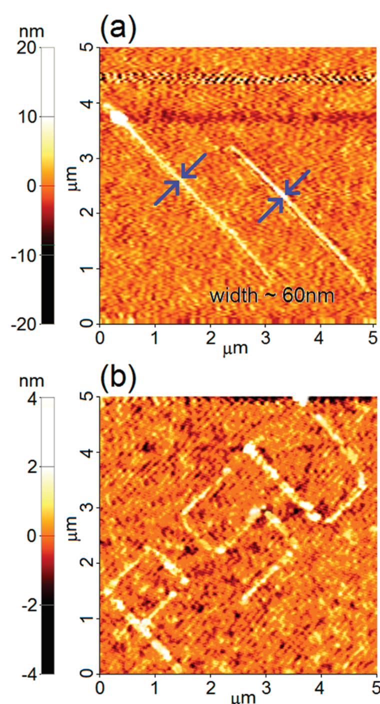


FIGURE 8. Topographic image (5 $\mu$m × 5 $\mu$m) of (a) line features with widths as small as about 60 nm (0.6 $\mu$N, 5 V), and (b) a pattern of the letters PSU (0.8 $\mu$N, 5 V). In the latter, the average line width is about 180 nm.

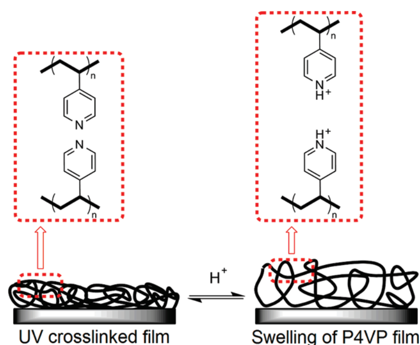


**FIGURE 9. Schematic suggesting that the swelling of P4VP thin film originated from the protonation of the pyridine units.**

A conventional DPN process involves two steps: (1) the ink molecules transport from the coated tip to the substrate through the water meniscus that naturally forms between them, and (2) ink is adsorbed via chemisorption or physical adsorption onto the surface to form any desired patterns (11, 19, 29). In our experiments, two major factors in controlling the properties of scribed patterns were found: the externally applied bias and tip-sample contact force. Comparison among the three patterns in Figure 3 indicates that higher bias voltages applied between the tip and the sample yield lines with increasing heights at a fixed contact force of 1.0 $\mu$N. The influence of applied bias on the feature's height was further verified at different contact forces. The same trend of the feature's height increase when applying greater external voltages was obtained, while the contact force was kept constant at 0.8 and 0.5 $\mu$N. As plotted in Figure 4a, a significant increase in the pattern's height is observed as the applied field strength is increased, indicating that the efficiency of acidic ion transport is electric-field dependent. Because of the presence of applied electric field, the electrostatic force acts as a driving force to facilitate the deposition of acidic ions into the polymer. Furthermore, because the patterning experiments were carried out in ambient conditions and the tip was initially dried with nitrogen, the electric field was required to facilitate the delivery of acidic ions into the substrate, so that the diffusive transport could occur consistently. In addition, the influence of Joule-heating discussed in electrostatic nanolithography was taken into consideration as well (30, 31). In the experiment presented above, no swollen pattern was obtained by using an uncoated tip when the tip was positively biased. This result indicates that the pattern formation cannot be attributed to the Joule heating alone. However, because the ion mobility is greatly enhanced when the temperature increases (32), we cannot completely eliminate the potential effect of Joule-heating. It could also be considered as a way to facilitate the ion transport.

Although electric fields has been utilized in electrochemical dip-pen nanolithography (E-DPN) (33), the role of electric field played in our approach differs from the one in E-DPN where metallic or semiconducting structures are fabricated via electrochemical reactions. By contrast, no electrochemical reaction is needed for fabricating patterns on P4VP films, the external electric field applied during the patterning process simply makes the surface patterning more reliable and repeatable.

Similar dependence of pattern height on contact force was found in our experiments: higher structures arose when using stronger contact force, which was in contrast to the report by Weeks et al. where the contact force had no effect on the structures (34). Figure 4b shows the dependencies of pattern height on contact force under different constant bias voltages. One can rationalize that the increase in the contact force exerted by the tip could lead to a greater tip area in contact with the polymer. It could also lead to a broadening of the liquid meniscus between the tip and the surface. Accordingly, the increase in pattern height upon increasing the contact force could be attributed to the wider tip-sample effective contact area, where a greater amount of acidic ions could be transported from the tip to the polymer.

A breakdown of polymer film did not take place under the applied electric fields (bias voltages were in the range of −5 to 5 V). Additionally, by monitoring the deflection of the AFM cantilever, no effect of external bias voltage on the vertical position of the tip was observed. This fact revealed that the electric force induced by the bias voltage can be eliminated as a potential factor for altering the tip-sample contact force. The high spring constant ($k$ = 40 N/m) of the non-contact AFM cantilevers used in our experiments (compared to general contact AFM probes) is important in achieving the precise control of contact forces during the patterning process.

The factors that affect the dimensions of the patterned features can be attributed but not limited to a combination of several variables, such as the writing speed (14, 34, 35), the effects of temperature and humidity (19, 34, 36), and the geometry and wettability of the tip (36). The dimensions of dot features as a function of the dwell time and relative humidity has been demonstrated in our previous work (26, 27). No structures could be created when the humidity was below 30%. It indicates that the transfer of hydronium ions in the acidic buffer takes place when sufficient liquid is present between the tip and the sample. Although the previous results indicate that humidity plays an effective role on the dot heights (27), its role in affecting feature size with this new electric field mechanism needs to be studied in a future work. Furthermore, it must be mentioned that the use of sharp tips was critical in achieving finer features. More studies focusing on line dimensions control with applied electric field are under way in our lab.

## CONCLUSIONS

We have provided evidence on the improved reliability and reproducibility of the electric-field-assisted DPN method for fabricating nanostructures on cross-linked P4VP thin films. Differing from a conventional DPN (where the patterns are created upon the accumulation of deposited ink molecules), electric-field-assisted DPN attains pattern formation as a result of the local protonation and subsequent swelling of P4VP films. A key aspect for improving the control over the patterning process constitutes the application of an

electric field between the tip and the sample. The acidic ions (i.e., $H_3O^+$) are more reliably transferred from the ink-coated tip to the polymer-covered substrate under the applied electric field. Well-defined features are generated due to the swelling of P4VP upon protonation of the pyridine units. The effects of patterning parameters, such as applied bias and contact force, were investigated. The results suggest that both a higher bias voltage and a stronger contact force result in a marked increase in the pattern height. Significantly, we demonstrated that the erasing of existing swollen structures on P4VP films can be achieved by taking advantage of the reversible property of pattern formation. The reversible characteristic of this patterning approach, and its operation requirement of very low voltages (in the −5 to 5 V range), can find applications in a variety of nanotechnologies that require feedback material response, including nanofluidics (where controlled variable size compartments can be used to selectively sort out molecules according to their size), and proton-based memory devices operating at very low voltages.

**Acknowledgment.** A.L.R. acknowledges support from the Oregon Nanoscience and Microtechnologies Institute through Grant N00014-08-1-1237. Xin Wang and M. Yan thank the financial supports from the National Institutes of General-Medical Science (NIGMS) under NIH Awards R01GM080295 and 2R15GM066279.

### REFERENCES AND NOTES

(1) Fulton, T. A.; Dolan, G. J. *Phys. Rev. Lett.* **1987**, *59*, 109.
(2) Tan, S. S.; Tang, Z. Y.; Liang, X. R.; Kotov, N. A. *Nano Lett.* **2004**, *4*, 1637.
(3) Santori, C.; Pelton, M.; Solomon, G.; Dale, Y.; Yamamoto, E. *Phys. Rev. Lett.* **2001**, *86*, 1502.
(4) Lundstrom, T.; Schoenfeld, W.; Lee, H.; Petroff, P. M. *Science* **1999**, *286*, 2312.
(5) Craighead, H. G. *Science* **2000**, *290*, 1532.
(6) Chao, C. Y.; Guo, L. J. *Appl. Phys. Lett.* **2003**, *83*, 1527.
(7) Piner, R. D.; Zhu, J.; Xu, F.; Hong, S. H.; Mirkin, C. A. *Science* **1999**, *283*, 661.
(8) Lee, K. B.; Park, S. J.; Mirkin, C. A.; Smith, J. C.; Mrksich, M. *Science* **2002**, *295*, 1702.
(9) Lim, J. H.; Mirkin, C. A. *Adv. Mater.* **2002**, *14*, 1474.
(10) Wang, H. T.; Nafday, O. A.; Haaheim, J. R.; Tevaarwerk, E.; Amro, N. A.; Sanedrin, R. G.; Chang, C. Y.; Ren, F.; Pearton, S. J. *Appl. Phys. Lett.* **2008**, *93*, 143105.
(11) Maynor, B. W.; Li, Y.; Liu, J. *Langmuir* **2001**, *17*, 2575.
(12) Demers, L. M.; Ginger, D. S.; Park, S. J.; Li, Z.; Chung, S. W.; Mirkin, C. A. *Science* **2002**, *296*, 1836.
(13) Ivanisevic, A.; Mirkin, C. A. *J. Am. Chem. Soc.* **2001**, *123*, 7887.
(14) Huang, C. Y.; Jiang, G. Q.; Advincula, R. *Macromolecules* **2008**, *41*, 4661.
(15) Maynor, B. W.; Li, J. Y.; Lu, C. G.; Liu, J. *J. Am. Chem. Soc.* **2004**, *126*, 6409.
(16) Anderson, M. S. *Anal. Chem.* **2005**, *77*, 2907.
(17) Yang, M.; Sheehan, P. E.; King, W. P.; Whitman, L. J. *J. Am. Chem. Soc.* **2006**, *128*, 6774.
(18) Cui, Y.; Wei, Q. Q.; Park, H. K.; Lieber, C. M. *Science* **2001**, *293*, 1289.
(19) Rozhok, S.; Piner, R.; Mirkin, C. A. *J. Phys. Chem. B* **2003**, *107*, 751.
(20) Hong, S. H.; Zhu, J.; Mirkin, C. A. *Langmuir* **1999**, *15*, 7897.
(21) Yan, M.; Harnish, B. *Adv. Mater.* **2003**, *15*, 244.
(22) Harnish, B.; Robinson, J. T.; Pei, Z. C.; Ramstrom, O.; Yan, M. *Chem. Mater.* **2005**, *17*, 4092.
(23) Tam, T. K.; Ornatska, M.; Pita, M.; Minko, S.; Katz, E. *J. Phys. Chem. C* **2008**, *112*, 8438.
(24) Privman, M.; Tam, T. K.; Pita, M.; Katz, E. *J. Am. Chem. Soc.* **2009**, *131*, 1314.
(25) Vaganova, E.; Meshulam, G.; Kotler, Z.; Rozenberg, M.; Yitzchaik, S. *J. Fluoresc.* **2000**, *10*, 81.
(26) Maedler, C.; Chada, S.; Cui, X.; Taylor, M.; Yan, M.; La Rosa, A. *J. Appl. Phys.* **2008**, *104*, 014311.
(27) Maedler, C.; Graaf, H.; Chada, S.; Yan, M.; Rosa, A. L.; Achim, W. *SPIE:* **2009**, *7364*, p 736409.
(28) Sader, J. E.; Chon, J. W. M.; Mulvaney, P. *Rev. Sci. Instrum.* **1999**, *70*, 3967.
(29) Senesi, A. J.; Rozkiewicz, D. I.; Reinhoudt, D. N.; Mirkin, C. A. *ACS Nano* **2009**, *3*, 2394.
(30) Lyuksyutov, S. F.; Paramonov, P. B.; Juhl, S.; Vaia, R. A. *Appl. Phys. Lett.* **2003**, *83*, 4405.
(31) Lyuksyutov, S. F.; Vaia, R. A.; Paramonov, P. B.; Juhl, S.; Waterhouse, L.; Ralich, R. M.; Sigalov, G.; Sancaktar, E. *Nat. Mater.* **2003**, *2*, 468.
(32) Cho, N.; Ryu, S.; Kim, B.; Schatz, G. C.; Hong, S. H. *J. Chem. Phys.* **2006**, *124*, 024714.
(33) Li, Y.; Maynor, B. W.; Liu, J. *J. Am. Chem. Soc.* **2001**, *123*, 2105.
(34) Weeks, B. L.; Noy, A.; Miller, A. E.; De Yoreo, J. J. *Phys. Rev. Lett.* **2002**, *88*, 255505.
(35) Jang, J. Y.; Hong, S. H.; Schatz, G. C.; Ratner, M. A. *J. Chem. Phys.* **2001**, *115*, 2721.
(36) Jang, J. Y.; Schatz, G. C.; Ratner, M. A. *J. Chem. Phys.* **2002**, *116*, 3875.

AM1005964